

## Statistics of Lyapunov exponent spectrum in randomly coupled Kuramoto oscillators

Soumen K. Patra and Anandamohan Ghosh

*Indian Institute of Science Education and Research Kolkata, Mohanpur, Nadia 741246, India*

(Received 22 July 2015; revised manuscript received 18 January 2016; published 7 March 2016)

Characterization of spatiotemporal dynamics of coupled oscillatory systems can be done by computing the Lyapunov exponents. We study the spatiotemporal dynamics of randomly coupled network of Kuramoto oscillators and find that the spectral statistics obtained from the Lyapunov exponent spectrum show interesting sensitivity to the coupling matrix. Our results indicate that in the weak coupling limit the gap distribution of the Lyapunov spectrum is Poissonian, while in the limit of strong coupling the gap distribution shows level repulsion. Moreover, the oscillators settle to an inhomogeneous oscillatory state, and it is also possible to infer the random network properties from the Lyapunov exponent spectrum.

DOI: [10.1103/PhysRevE.93.032208](https://doi.org/10.1103/PhysRevE.93.032208)

The sensitivity of a dynamical system to small changes in the initial conditions is typically quantified by estimating the *Lyapunov exponents* (LE). LEs quantify the temporal growth of a perturbation in phase space and if the maximal Lyapunov exponent is positive the corresponding dynamics is *chaotic* [1]. In the case of  $N$ -dimensional spatially extended systems, it is possible to compute the  $N$ -dimensional Lyapunov spectrum (LS) and important physical quantities like the Lyapunov dimension [2], Kolmogorov-Sinai entropy [3], synchronization criteria [4], extensive or subextensive properties [5], etc. can be determined. These coarse-grained quantities along with the scaling behavior of the LS are useful tools in characterization of chaotic systems. However, there have been fewer attempts to extract more information about the topology of the dynamical system from the full LS.

In an earlier attempt, the LS computed for a coupled map lattice model was shown to exhibit synchronization induced by disorder [6]. Another significant observation had been that this LS can be compared with the energy spectrum of a Hermitian operator showing disorder-induced localization as in the Anderson problem [6,7]. The comparison is justified, if we observe that the computation of the LEs, essentially involving the diagonalization of the Jacobian matrix, is analogous to determining the energy spectrum of discrete Schrödinger operators in quantum systems. Furthermore, recall that in the Anderson localization problem depending on the strength of the on-site disorder term, a transition from localized to extended states is also observed. For example, in the well-studied Harper model, the energy gap distribution shows a transition from Poisson to Wigner distribution as predicted by the random matrix theory [8,9]. While this property is conjectured to be an universal signature of *quantum chaos* [10] can there be evidence of avoided level crossing in simple classical systems?

In coupled one-dimensional maps it is known that differences in the Lyapunov exponents exhibit *coupling sensitivity of chaos* [11]. It has also been shown that in chaotic coupled maps the LEs exhibit avoided level crossings and level spacing distribution is exponentially suppressed at small values [12]. The important observation made in Ref. [12] is that the disordered chaotic systems have randomness due to two sources, namely, quenched disorder and chaotic fluctuations. However, interesting spatiotemporal patterns arise in quenched dynamical systems even in the absence of chaotic behavior

[13]. It will be interesting to study how quenched disorder influences the behavior of the level spacing distribution in large coupled systems in the absence of *dynamic randomness*. In this paper, we explore the spectral properties of the LS of a system of randomly coupled phase oscillators evolving continuously in time. We find that the LE spectral statistics depend on the random network properties and show signatures of *level repulsion* in close analogy to the Anderson problem. We demonstrate that for weak and strong coupling strengths the distribution of LE differences exhibit Poisson and Wigner distributions, respectively.

The motivation for studying the dynamics on a random network is manifold. The short-ranged, long-ranged, power-law, scale-free, or random connectivity properties of such networks are manifested in the emergent behavior of the dynamical processes taking place on them [14]. Synchronized dynamics is one such behavior and the onset of synchronization or the lack of it as a function of the topological property of the network has been a subject of active research [4,15]. A paradigmatic model for studying synchronization is the Kuramoto model, a system of globally coupled phase oscillators that depending on the strength of coupling exhibits emergence of synchronized behavior [16,17]. The Kuramoto model consists of  $N$  coupled oscillators, in which the phase of the oscillators evolves in time according to

$$\frac{d\theta_n}{dt} = \omega_n + \frac{K}{N} \sum_{m=1}^N \sin(\theta_m - \theta_n), \quad (1)$$

where  $n = 1, 2, \dots, N$  is the oscillator index and each oscillator is coupled to all other oscillators.  $\theta_n$  is the phase of the  $n$ th oscillator and  $K \geq 0$  is the coupling constant. Each oscillator has an intrinsic natural frequency,  $\omega_n$ , randomly drawn from a given probability density  $g(\omega)$ . The Kuramoto model has been mostly studied for a unimodal frequency distribution  $g(\omega)$ , with mean frequency  $\omega = \omega_0$  [17,18]. In this study the frequencies will be chosen from a Lorentzian distribution. It is known that in the limit  $N \rightarrow \infty$ , the system of oscillators in the steady state undergoes a continuous transition at the critical threshold  $K_c = 2/\pi g(0)$ . For  $K < K_c$ , each oscillator tends to oscillate independently with its own natural frequency. On the other hand, when  $K > K_c$ , the coupling synchronizes the phases of the oscillators, and in the limit  $K \rightarrow \infty$ , they all oscillate with the mean frequency  $\omega_0$ .

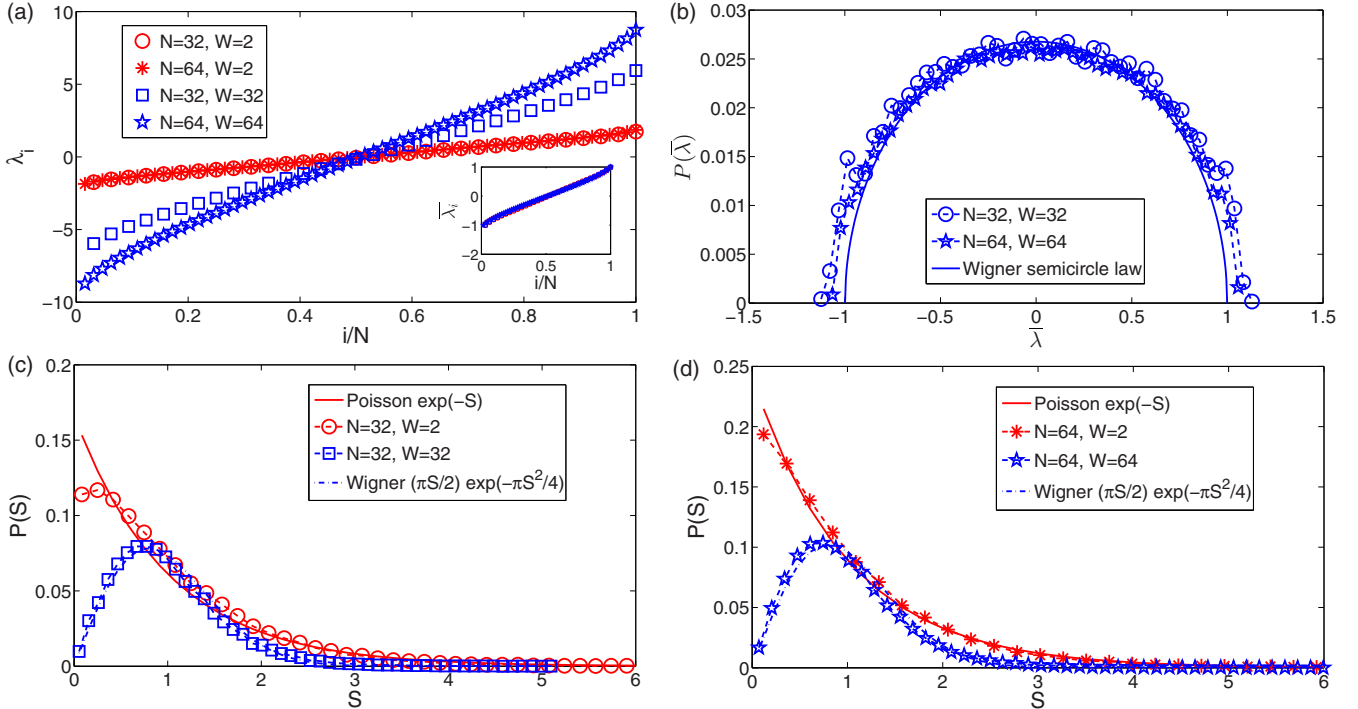


FIG. 1. Eigenvalue statistics of random uniform matrix. (a) Eigenvalue spectrum of banded coupling matrix,  $\lambda_i$  vs  $i/N$ , shown for two system sizes,  $N = 32, 64$  and  $W = 2, N$ . The eigenvalue spectrum is symmetric and the rescaled values  $\tilde{\lambda}_i = 2\lambda_i / (\lambda_{\max} - \lambda_{\min})$  exhibit data collapse as shown in inset. (b) The distributions of rescaled eigenvalues show agreement with Wigner semicircle law. (c) The eigenvalue gap distribution  $P(S)$ , where  $S$  is the gap between successive eigenvalues are shown for band-widths  $W = 2, N$ , where  $N = 32$ . The continuous curves are theoretical predictions. (d) Same as (c) for  $N = 64$ . An ensemble average is taken over for 1000 realizations.

Recent studies on the Kuramoto model and its many variants have focused on the onset of synchronization in large networks coupled by random connectivity matrices [18]. The transition from incoherence to coherence can be captured by a suitably defined order parameter and the critical coupling strength depends on the largest eigenvalue of the connectivity matrix, called the coupling matrix [19]. Mean-field behavior with such mixed interactions has also been recently studied under conditions of very general randomness [20,21]. In our variant of the Kuramoto model, we consider coupling matrix elements to be uniformly distributed random numbers with zero mean. This implies that both attractive or repulsive interactions are encoded in a random coupling matrix  $A_{nm}$ , and the Kuramoto model now assumes the form

$$\frac{d\theta_n}{dt} = \omega_n + \frac{K}{W} \sum_{m=1}^N A_{nm} \sin(\theta_m - \theta_n), \quad (2)$$

where  $A_{nm} = 0$ , for  $|n - m| \geq W$ , i.e., for any  $W < N$ , the coupling matrix is banded. In the case of all-to-all coupling ( $W = N$ ), the random connections introduce frustration in the system leading to *quasientrapment* with slow relaxation as in a glassy system [22]. However, there is some discrepancy in determining the critical value at which the transition takes place and also the exact nature of the relaxation dynamics of Eq. (2) is debated [18,22,23]. In recent studies [19], the elements of the coupling matrix are randomly chosen 0 or 1 and the critical transition is found to take place at

$K_c^* = K_c / \lambda_{\max}$ , where  $\lambda_{\max}$  is the largest eigenvalue of the random coupling matrix. While the above-mentioned studies address important issues of relaxation dynamics and the onset of synchronization, we are interested in inferring the random network topology from the dynamics of the oscillator network.

Let us now consider a random coupling matrix  $A_{nm}$ ,  $n, m = 1, 2, \dots, N$ , where the elements are chosen from a uniform random distribution in the domain  $[-1, 1]$ . The ensemble of such random matrices, in the limit of large  $N$ , shows universal properties [9]. One such signature in the case of symmetric matrices is that the eigenvalue distribution follows a semicircle law [24]. This can be easily verified for an ensemble of random matrices and shown in Fig. 1(b). Another universal feature is that the eigenvalue spacing distribution computed from an ensemble of random matrices shows Wigner distribution [9,24]. If the spacings are denoted by  $S$ , the distribution  $P(S) = \frac{\pi S}{2} \exp(-\pi S^2/4)$ . This is known as Gaussian orthogonal ensemble (GOE) and the numerical estimates along with theoretical curves are shown in Figs. 1(c) and 1(d) for two system sizes  $N = 32, 64$ , respectively. These random matrices correspond to the case of all-to-all coupling [ $W = N$  in Eq. (2)]. As mentioned earlier the coupling matrices can also be banded, with bandwidth  $W$ , corresponding to short-range coupling. In the case when  $W = 2$ , i.e., only the tridiagonal matrix elements survive, all the eigenvalues will be completely independent of each other leading to a Poissonian spacing distribution  $P(S) \sim \exp(-S)$  [see solid curves in Figs. 1(c) and 1(d)]. This limit

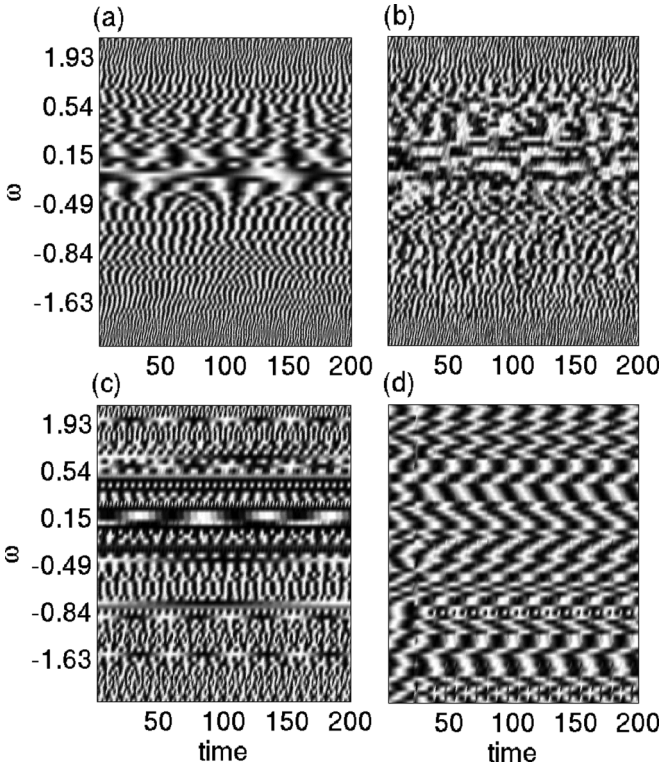


FIG. 2. Spatiotemporal dynamics of  $\sin(\theta(\omega_i, t))$  for randomly coupled Kuramoto oscillators ( $N = 64$ ). The oscillator index is ordered according to the magnitude of the frequency. (a)  $K = 2$ ,  $W = 2$ , (b)  $K = 2$ ,  $W = N$ , (c)  $K = 100$ ,  $W = 2$ , (d)  $K = 100$ ,  $W = N$ .

corresponds to the case of completely disordered systems. For any banded matrix,  $1 < W < N$ , it is expected that there is transition from Poissonian statistics to Wigner statistics. It has been rigorously ascertained that  $W_c \sim \sqrt{N}$ , is the critical bandwidth, below (above) which eigenvalue spectrum is Poissonian (Wigner) [25]. It is to be noted that the eigenvalue spectrum irrespective of  $N$  and  $W$  are indistinguishable up to a scaling factor [inset of Fig. 1(a)], but the eigenvalue spacing distribution reveals the distinct structure of the random matrices.

Now we will study the dynamics of the random Kuramoto model. The coupled differential equations, Eq. (2), are numerically integrated by Runge-Kutta fourth-order method with a time step of  $10^{-2}$ . The spatiotemporal evolution is shown in Fig. 2 for different choices of  $K$  and  $W$ . In the spatiotemporal plots the oscillator index is ordered according to the strength of the intrinsic frequencies,  $\omega_i$  drawn from a Lorentzian distribution  $g(\omega) = \frac{\gamma}{\pi(\gamma^2 + \omega^2)}$ . We have set  $\gamma = 1$ , such that the critical coupling for onset of synchronization in the traditional Kuramoto model is  $K_c = 2$ . Let us first consider the case of strong coupling  $K = 100$  and the ranges of coupling  $W = 2$  and  $W = N = 64$ , for which the spatiotemporal dynamics are shown in Figs. 2(c) and 2(d), respectively. Each snapshot in time indicates inhomogeneous spatial state and we have checked that the spatial correlations decay exponentially. However, in the case of global coupling, the temporal evolution shows periodic recurrence of the inhomogeneous spatial states. Figures 2(a) and 2(b) correspond to weak coupling,  $K = 2$ , showing spatial inhomogeneity and chaotic evolution. While

understanding the onset of synchronization has been one of the primary goals in studying the traditional Kuramoto model and its variants, the spatiotemporal dynamics in our model do not indicate any synchronized behavior. The disorder in the coupling introduces frustration resulting in spatial inhomogeneity. The extent of synchronization is typically captured by a complex order parameter defined as

$$\mathbf{r}(t) = r(t)e^{i\psi(t)} = \frac{1}{N} \sum_{m=1}^N e^{i\theta_m(t)}, \quad (3)$$

where  $r(t)$  with  $0 \leq r(t) \leq 1$  measures the phase coherence of the oscillators, while  $\psi(t)$  gives the average phase. In the case of random coupling as in Eq. (2) it will be more appropriate to define a local order parameter weighted by the random coupling matrix,

$$\mathbf{z}_n(t) = z_n(t)e^{i\phi_n(t)} = \frac{1}{N} \sum_{m=1}^N A_{nm} e^{i\theta_m(t)}. \quad (4)$$

However, for the random coupling matrix we consider here, either of the order parameters are inadequate to describe the irregular spatiotemporal dynamics and this motivates us to compute the Lyapunov spectrum to characterize the random Kuramoto model.

For a general  $N$ -dimensional dynamical system  $\dot{\theta}_i(t) = f(\theta_1(t), \theta_2(t), \dots, \theta_N(t))$  the dynamics of small perturbations is given by the linearized system  $\delta\dot{\theta}_i = J\delta\theta_i$ , where  $J$  is the Jacobian matrix. The solution of the linearized system can be represented in matrix form as  $\delta\theta(t) = M(t)\delta\theta(0)$ . The LEs  $\{\Lambda_1, \Lambda_2, \dots, \Lambda_N\}$  defined as

$$\Lambda = \lim_{t \rightarrow \infty} \frac{1}{t} \log \frac{\|\delta\theta(t)\|}{\|\delta\theta(0)\|} \quad (5)$$

can be equivalently computed from the logarithm of the eigenvalues of the Osledec matrix  $\lim_{t \rightarrow \infty} [M(t)^T M(t)]^{(1/2t)}$ .

We compute the LE based on an algorithm involving the continuous Gram-Schmidt orthonormalization [26]. This method is particularly efficient in the presence of degeneracy of eigenvalues as compared to other standard methods [27]. We

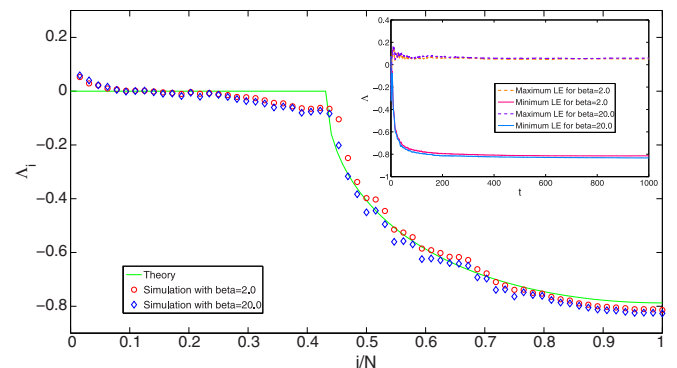


FIG. 3. The Lyapunov spectrum for the Kuramoto oscillators with normally distributed frequencies. The theoretical curve [28] and the numerical simulation results for two stability parameter values ( $\beta = 2, 20$ ) are shown for a single realization. The numerical integration has been done for  $N = 64$  oscillators with a step size of  $10^{-2}$  and  $10^5$  time steps. Inset shows the convergence of the maximum and the minimum LE for a single realization.

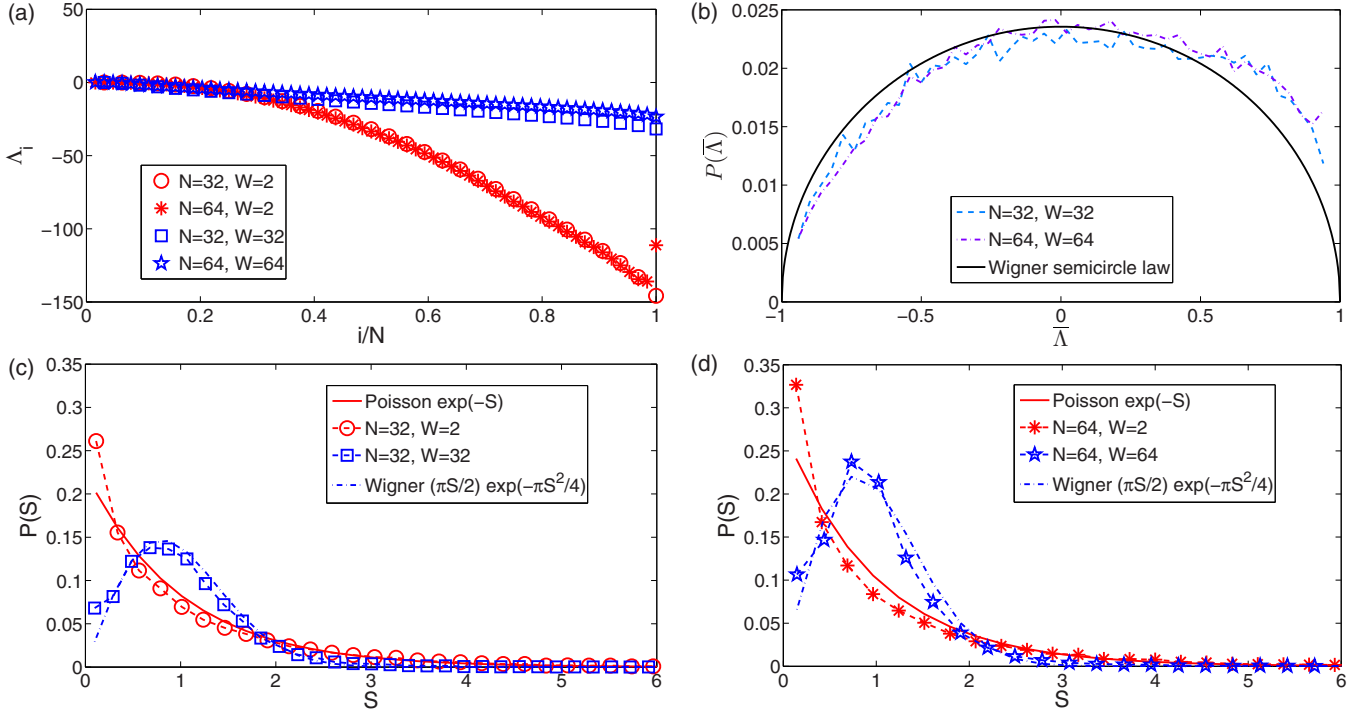


FIG. 4. Lyapunov exponent statistics of randomly coupled Kuramoto oscillators for strong coupling,  $K = 100$ . (a) Lyapunov spectrum of banded coupling matrix,  $\Lambda_i$  vs  $i/N$ , shown for two system sizes,  $N = 32, 64$  and  $W = 2, N$ . (b) The distributions of rescaled Lyapunov exponents  $\bar{\Lambda}_i$ , where the rescaled values  $\bar{\Lambda}_i = (2\Lambda_i + |\Lambda_{\min}|)/|\Lambda_{\min}|$ . (c) The Lyapunov exponent gap distribution  $P(S)$ , where  $S$  is the gap between successive Lyapunov exponents are shown for bandwidths  $W = 2, N$ , where  $N = 32$ . The continuous curves are theoretical predictions. (d) Same as (c) for  $N = 64$ . An ensemble average is taken over for  $\sim 2 \times 10^3$  realizations.

first validate the numerical method for the analytically solvable case of Kuramoto oscillators with constant coupling. In the presence of Gaussian frequency distribution the analytical expression of the Lyapunov spectrum is given in Ref. [28], which is in reasonable agreement with our numerical estimates considering that our simulation has been done for  $N = 64$  oscillators while the theoretical curve corresponds to  $N \rightarrow \infty$  limit (Fig. 3). For estimating the LS we use the algorithm proposed in Ref. [26], which involves a stability parameter  $\beta$ . In Fig. 3 the numerical computations of LEs have been done with  $\beta = 2, 20$  and both data are almost equal, indicating robust convergence of the LS. In all our simulation results, shown henceforth, the stability parameter,  $\beta$ , has been chosen such that it is greater than the magnitude of all LEs,  $\beta > \max(\text{abs}(\Lambda))$ .

Now we compute the LS for randomly coupled Kuramoto oscillators. In Fig. 4(a) we show the LS for large coupling strength, indicating that the dynamics is not chaotic (all LE being negative). However, more information can be obtained from the spectrum and this is the main focus of this paper. The distribution of the rescaled LE is computed for strong coupling strength,  $K = 100$ , and for all-to-all coupling ( $W = N$ ) is shown in Fig. 4(b) along with the Wigner semicircle law for comparison. The LE gap distribution indicates Wigner statistics for all-to-all coupling  $W = N$  while the distribution is Poissonian for bandwidth of the coupling matrix  $W = 2$ . Recall that these statistics are similar to that observed for the coupling matrices (Fig. 1). It is important to note that numerical data agrees well with the theoretical functions and it does not involve any fitting. The distributions are only normalized such

that

$$\int P(S)dS = 1 \quad \text{and} \quad \int SP(S)dS = 1.$$

The LE statistics also exhibits a transition from Poissonian to Wigner distribution at  $\approx W_c$ , the critical band width of the coupling matrix. This transition can be quantified in terms of the parameter  $\alpha$  of the Brody distribution [29] defined as

$$P(S) = (\alpha + 1)bS^\alpha \exp(-bS^{\alpha+1}), \tag{6}$$

where

$$b = \left[ \Gamma\left(\frac{\alpha + 2}{\alpha + 1}\right) \right]^{\alpha+1}. \tag{7}$$

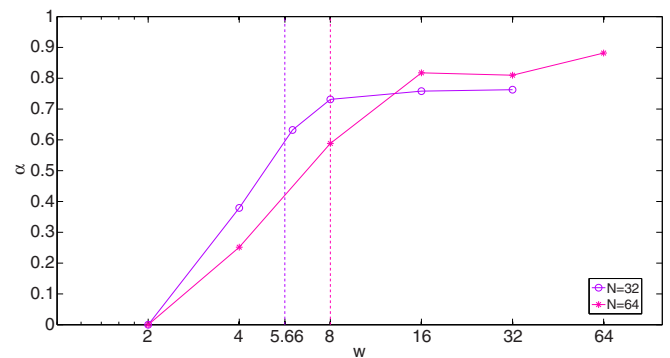


FIG. 5. The Brody parameter  $\alpha$  is shown for varying matrix bandwidth  $W$ . The coupling strength  $K = 100$ .

The parameter  $\alpha \in [0, 1]$  parameterizes the Brody distribution and it is easy to see that  $\alpha = 0$  corresponds to Poisson distribution and  $\alpha = 1$  corresponds to Wigner distribution. The Brody parameter  $\alpha$  is determined by fitting Eq. (6) to  $P(S)$  obtained for varying matrix bandwidth  $W$ . (The fitting is done in MATLAB using the Levenberg-Marquardt method.) Below the critical band-width of the coupling matrix ( $W < W_c = \sqrt{N} \approx 5.65$ ) for  $N = 32$  the LS gap distribution is Poissonian ( $\alpha = 0$ ,  $W = 2$ ) and for  $W > W_c$  the value of  $\alpha$  is closer to 1 confirming level repulsion as expected for Wigner distribution (Fig. 5). Similar transition is seen for  $N = 64$  at  $W \approx 8$ .

Next we investigate the role of weak coupling. It is expected that for small coupling, (say,  $K = 5$ ), there are fewer frequencies that satisfy  $|\omega_n| < KNz_n/W$ . The frequencies that satisfy this condition exhibit phase locking while the remaining number of oscillators are drifting. In Figs. 2(a) and 2(b) the spatiotemporal dynamics are shown for  $W = 2$  and  $W = N = 64$ , respectively. The LS and the LE statistics are computed for  $K = 5$  and shown in Fig. 6. In the case of weak coupling for bandwidth  $W = 2$ , the LE,  $\Lambda_i \leq 0$ , and the corresponding spacing distribution resembles Poisson distribution as shown in Fig. 6(c). While for weak and all-to-all coupling the spatiotemporal dynamics has a significant number of positive and zero LE, corresponding to the chaotic and the drifting oscillators, respectively. The zero LEs in the spectrum contribute to the sharp peak in  $P(S)$  as the gap  $S \rightarrow 0$ . The spacing distributions are also computed separately for positive

and negative LEs showing level clustering as seen in Fig. 6(d). In the case of all-to-all coupling if we now vary the coupling strength,  $K$ , the number of chaotic and drifting oscillators decreases with increase in the coupling strength  $K$ . In the absence of chaotic fluctuations the coupling disorder prevails, resulting in enhanced level repulsion due to strong coupling. We observe that for moderate values of  $K \approx 30$ ,  $N = 32$  and  $K \approx 50$ ,  $N = 64$  the statistics show sharp peaks. However, the LS converges to Wigner like distribution for coupling strength  $K \geq 100$ . We show the spacing distributions  $P(S)$  in Fig. 7 and to quantify the resemblance to the Wigner distribution the estimated Brody parameter is shown for varying  $K$  (inset of Fig. 7). Thus, for strong all-to-all coupling the spatiotemporal dynamics is most sensitive to the properties of the coupling matrix.

In the Kuramoto model in Eq. (2) if we set  $\omega_i = 0$  and add a noise term we obtain the XY spin-glass model [30], which shows a paramagnetic spin-glass transition. Level spacing distribution in spin-glass model or in a quantized version of Kuramoto oscillators are worth investigating. In order to explore the generality of our method we have investigated a related model, a system of classical XY rotors with infinite range coupling known as Hamiltonian mean field model (HMF) [31]. The HMF is described by the Hamiltonian

$$H = \sum_{i=1}^N \frac{p_i^2}{2} + \frac{K}{2N} \sum_{i,j=1}^N A_{ij} [1 - \cos(\theta_i - \theta_j)], \quad (8)$$

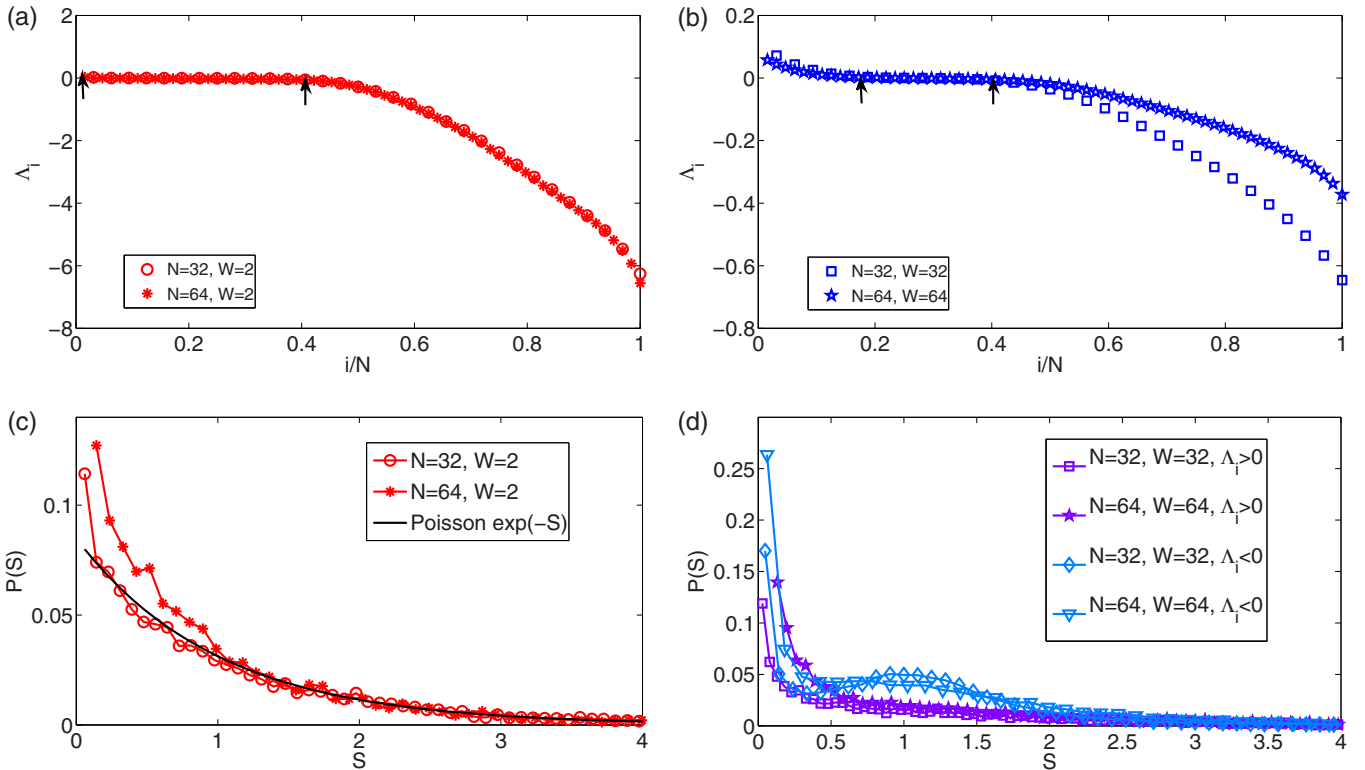


FIG. 6. Lyapunov exponent statistics of randomly coupled Kuramoto oscillators for weak coupling,  $K = 5$ . Lyapunov spectrum of banded coupling matrix,  $\Lambda_i$  vs  $i/N$ , is shown for two system sizes,  $N = 32, 64$  for bandwidth (a)  $W = 2$ , (b)  $W = N$ . The LS is an ensemble average taken over for  $\sim 10^3$  realizations. The arrows indicate the range in which the LEs are  $\sim 0$ . (c) The spacing distribution for  $\Lambda_i < 0$  is shown for  $W = 2$ . In (d) the spacing distributions are shown separately for positive and negative LS for  $W = N$ .

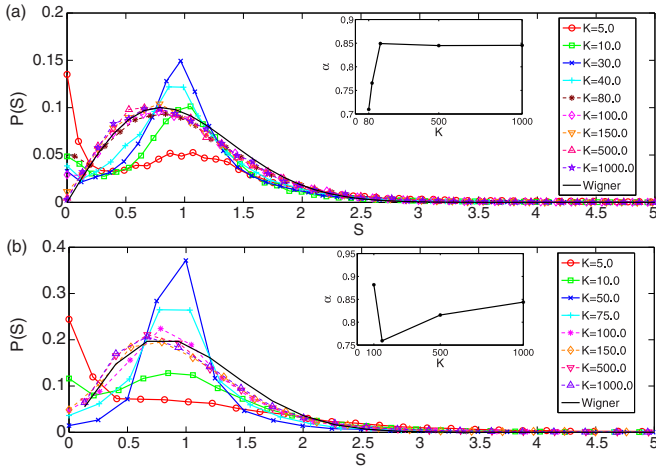


FIG. 7. Lyapunov exponent statistics of randomly all-to-all coupled Kuramoto oscillators for varying coupling strength  $K$  for system size (a)  $N = 32$ , (b)  $N = 64$ . The ensemble averages are taken over  $\sim 10^3$  realizations. The insets show the estimated Brody parameter as a function of  $K$ .

where  $N$  particles are moving on a circle  $\theta_i \in [-\pi, \pi]$  and  $p_i$  are the corresponding momenta. The HMF model, for homogeneous coupling, i.e.,  $A_{ij} = 1 \forall i, j$ , is analytically tractable and a phase transition from ordered to disordered state is seen as a function of the energy per particle,  $U$ . For,  $K > 0$  ( $K < 0$ ), particles attract (repel) resembling the ferromagnetic (anti-ferromagnetic) state. For the ferromagnetic case the maximal LE characterizes the transition from ordered to disordered state. The HMF model is integrable at small and large  $U$ , i.e., in these limits the maximum LE vanishes, while the system is

most chaotic at  $U_c \approx 0.75$  [ as seen in Fig. 8(a)]. In our study, we have introduced a random coupling matrix  $A_{ij}$ , whose elements are chosen from a uniform distribution in  $[-1, 1]$ , and obtained the LS and the spacing distribution as shown in Fig. 8. The signature of level-repulsion in HMF model is evident at  $U = 1 \approx U_c$ , reminiscent of Wigner distribution seen in level spacing statistics of Harper equation at criticality [8]. For  $U = 10 \gg U_c$ , i.e., the system is integrable and the LS statistics resembles Poisson distribution. We have also quantified the similarity by estimating the parameter  $\alpha$  of the Brody distribution and have found  $\alpha = 0$  and  $\alpha = 0.9543$  for  $U = 10$  and  $U = 1$ , respectively.

Our results show that the coupling sensitivity of coupled oscillator systems is remarkably captured by level spacing distribution of Lyapunov exponents in dissipative as well as conservative dynamical systems. The simple numerical analysis presented here suggests a novel method of characterization of complex spatiotemporal systems. The sensitivity to coupling matrix results in level repulsion as observed in disorder-induced localization in quantum systems. In the random Kuramoto model with local coupling  $W = 2$  ( $W < \sqrt{N}$ ) the coupling matrix is tridiagonal (narrow band) and the corresponding distribution is Poissonian irrespective of the coupling strength. On the other hand, for strong and all-to-all coupling the repulsion is stronger and the level statistics resembles Wigner distribution. Earlier studies on coupled chaotic maps showed that depletion in the distribution of LE spacings is exponential at small spacings [12]. In contrast to the chaotic dynamics of the low-dimensional coupled maps, in our study the resemblance to Wigner distribution is exclusively exhibited by the negative LEs. In the absence of dynamic randomness the LS only depends on the quenched

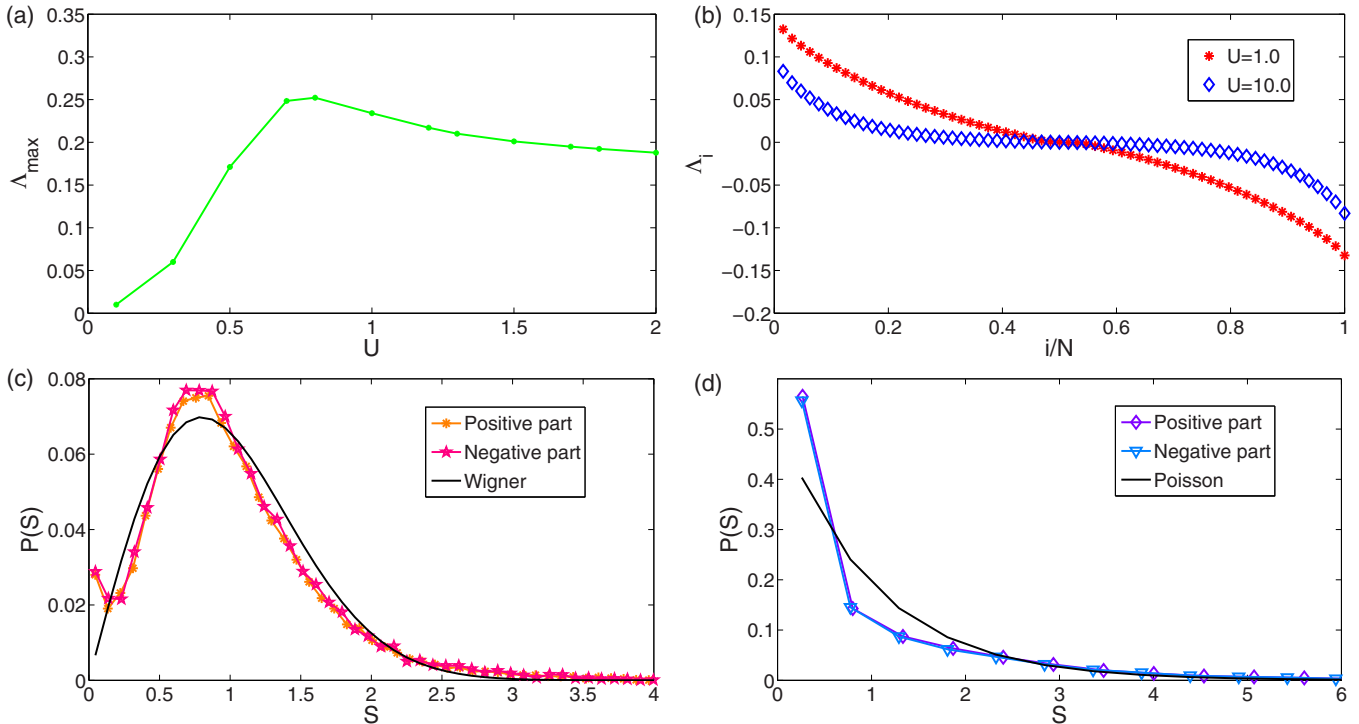


FIG. 8. Lyapunov exponent statistics of randomly coupled HMF model ( $N = 32$ ). (a) The largest LE as a function of the energy per particle  $U$ . (b) LS shown for  $U = 1, 10$ . The LS spacing distributions, for the positive and the negative LEs, are shown for (c)  $U = 1.0$ , (d)  $U = 10.0$ .

disorder, i.e., the statistical properties of the random coupling matrix. Our preliminary results also show similar repulsion in random HMF model, which is governed by different physics and needs to be studied in detail. However, the process of estimating the full LS is computationally intensive and all our

results being averaged over a large number of realizations of random matrices puts a restriction on us exploring large system sizes. Determining the finite-size effects and establishing whether our findings are truly universal need to be further investigated.

- 
- [1] J. P. Eckmann and D. Ruelle, *Rev. Mod. Phys.* **57**, 617 (1985).
- [2] P. Fredrickson, J. L. Kaplan, E. D. Yorke, and J. A. Yorke, *J. Diff. Equat.* **49**, 185 (1983).
- [3] I. P. Cornfeld, S. F. Fomin, and Ya. G. Sinai, *Ergodic Theory* (Springer-Verlag, Berlin, 1982).
- [4] A. Pikovsky, M. Rosenblum, and J. Kurths, *Synchronization: A Universal Concept in Nonlinear Sciences* (Cambridge University Press, Cambridge, 2003), Vol. 12.
- [5] K. A. Takeuchi, H. Chaté, F. Ginelli, A. Politi, and A. Torcini, *Phys. Rev. Lett.* **107**, 124101 (2011).
- [6] S. Isola, A. Politi, S. Ruffo, and A. Torcini, *Phys. Lett. A* **143**, 365 (1990).
- [7] P. W. Anderson, *Phys. Rev.* **109**, 1492 (1958).
- [8] P. G. Harper, *Proc. Phys. Soc. London, Sect. A* **68**, 874 (1955).
- [9] M. L. Mehta, *Random Matrices* (Elsevier/Academic Press, Amsterdam, 2004).
- [10] F. Haake, *Quantum Signatures of Chaos* (Springer, Berlin/Heidelberg/New York, 2000).
- [11] H. Daido, *Prog. Theor. Phys.* **72**, 853 (1984).
- [12] V. Ahlers, R. Zillmer, and A. Pikovsky, *Phys. Rev. E* **63**, 036213 (2001).
- [13] A. R. Bishop, K. Fesser, P. S. Lomdahl, W. C. Kerr, M. B. Williams, and S. E. Trullinger, *Phys. Rev. Lett.* **50**, 1095 (1983).
- [14] R. Albert and A. L. Barabási, *Rev. Mod. Phys.* **74**, 47 (2002).
- [15] M. Timme, *Phys. Rev. Lett.* **98**, 224101 (2007).
- [16] Y. Kuramoto, in *International Symposium of Mathematical Problems in Theoretical Physics*, edited by H. Araki, Lecture Notes in Physics Vol. 39 (Springer, Berlin, 1975).
- [17] S. H. Strogatz, *Physica D* **143**, 1 (2000).
- [18] J. A. Acebrón, L. L. Bonilla, C. J. Pérez Vicente, F. Ritort, and R. Spigler, *Rev. Mod. Phys.* **77**, 137 (2005).
- [19] J. G. Restrepo, E. Ott, and B. R. Hunt, *Phys. Rev. E* **71**, 036151 (2005).
- [20] H. Hong and S. H. Strogatz, *Phys. Rev. E* **85**, 056210 (2012).
- [21] D. Iatsenko, P. V. E. McClintock, and A. Stefanovska, *Nat. Commun.* **5**, 4118 (2014).
- [22] H. Daido, *Phys. Rev. Lett.* **68**, 1073 (1992).
- [23] J. C. Stiller and G. Radons, *Phys. Rev. E* **58**, 1789 (1998).
- [24] E. Wigner, *Ann. Math.* **67**, 325 (1958).
- [25] L. Erdos and A. Knowles, *Annales Henri Poincaré* (SP Birkhäuser Verlag, Basel, 2011), Vol. 12, p. 1227; L. Erdos, A. Knowles, H. T. Yau, and J. Yin, *Commun. Math. Phys.* **323**, 367 (2013).
- [26] F. Christiansen and H. H. Rugh, *Nonlinearity* **10**, 1063 (1997).
- [27] G. Benettin, L. Galgani, and J. M. Strelcyn, *Phys. Rev. A* **14**, 2338 (1976); I. Shimada and T. Nagasama, *Prog. Theor. Phys.* **61**, 1605 (1979).
- [28] G. Radons, in *Disordered Dynamical Systems*, edited by G. Radons, W. Just, and P. Häussler, Collective Dynamics of Nonlinear and Disordered Systems (Springer, Berlin, 2005).
- [29] T. A. Brody, *Lett. Nuovo Cimento* **7**, 482 (1973); T. Prosen and M. Robnik, *J. Phys. A* **27**, 8059 (1994).
- [30] D. Sherrington and S. Kirkpatrick, *Phys. Rev. Lett.* **35**, 1792 (1975).
- [31] T. Dauxois, V. Latora, A. Rapisarda, S. Ruffo, and A. Torcini, *Dynamics and Thermodynamics of Systems with Long-Range Interactions* (Springer, Berlin/Heidelberg, 2002).